

ARCTIC HAZE, MERCURY AND THE CHEMICAL COMPOSITION OF SNOW ACROSS NORTHWESTERN ALASKA

Thomas A. Douglas and Matthew Sturm

U. S. Army Cold Regions Research and Engineering Laboratory
Post Office Box 35170, Fort Wainwright, Alaska 99703-0170

Thomas.A.Douglas@erdc.usace.army.mil; msturm@crrel.usace.army.mil

Abstract

We sampled three layers of snow at 16 sites along a 1200 km transect from Nome to Barrow across northwestern Alaska. Samples were analyzed for major element concentrations, specific conductance and pH. Samples from 5 of the sites were analyzed for trace element concentrations. Pb, Cd, SO_4^{2-} and non-sea salt SO_4^{2-} concentrations were significantly higher in layers deposited later in the winter than those deposited earlier. This is consistent with the seasonal increase in atmospheric aerosol loading (arctic haze) that develops as the Arctic polar front expands southward in March and April. Haze contaminant concentrations in the snow pack were as high south of the Brooks Range as they were to the north, suggesting the Brooks Range is not an effective orographic barrier to aerosol transport. Computed yearly non-sea salt SO_4^{2-} loading rates at the 16 sites ranged from 12 to 281 $\text{mg/m}^2/\text{yr}$. Elevated concentrations of Hg, Na and Cl were measured near the Arctic Ocean coast but not near the Bering Sea coast. To explain this pattern we suggest that the “effective distance from the coast,” inferred from prevailing wind directions and storm tracks, is critical in governing whether halogen emissions from the ocean are available for photochemical reactions that result in Hg deposition in the snow.

Key words: Arctic, snow chemistry, trace elements, aerosols

INTRODUCTION

An important source of environmental contaminants in northwest Alaska is arctic haze. During late winter and early spring, when the Polar Front extends southward and a cold dry air mass blankets the Arctic, Eurasian industrial emissions migrate into the Arctic Basin where they accumulate (Shaw, 1995; Polissar et al., 1998a, 1999). When present, they color the atmosphere, making it look dingy or hazy, hence the name (Mitchell, 1956). These aerosol contaminants reach their maximum concentration in late winter (Rahn et al., 1977; Rahn, 1981; Barrie and Hoff, 1985; Barrie, 1986; Bodhaine, 1989; Herbert et al., 1989; Cheng et al., 1993; Xie et al., 1999; Polissar et al., 2001) and decline in the spring (Fig. 1A) when the sun returns and the warm, moisture-laden Pacific Ocean air mass begins to displace the Polar Front northward. The seasonal concentration of aerosols matches the build up of the arctic snow pack, with the maximum haze concentration occurring at about the same time the snow pack reaches maximum depth (Fig. 1B).

It is known that haze contaminants end up in arctic ecosystems (Oehme and Ottar, 1984; AMAP, 1997, Xie et al., 1999), but how and when they are scavenged from the atmosphere is complex and not fully understood (Dominé and Shepson, 2002). Because the increase in haze concentration through the winter closely mirrors the build up of the snow pack, and because the concentration declines before the snow has fully melted, it is probably safe to assume that most haze-derived contaminants first enter the ecosystem by being deposited in the snow. Both wet and dry deposition contribute to this process, but wet deposition appears to be many times more effective at scavenging aerosols than dry deposition. Studies have shown that rain and snow account for up to 90% of the pollutant and dust scavenging that occurs in the Arctic lower atmosphere (Uematsu et al., 2000), while in Greenland 60 to 90% of all SO_4^{2-} deposited in the snow pack was found to be the result of wet deposition by snowfall (Bergin et al., 1995; Davidson et al., 1989).

In principle, the snow pack also contains a temporal record of the same loading because each snow layer preserves within itself the nonvolatile aerosols scavenged from the air mass at the time it was

deposited. In essence the layered snow pack is a stack of “snap-shots” of the aerosol loading throughout the winter. This record may, in fact, be as important as the record of what is in the atmosphere because it is a direct measure of the amount transferred to the environment. Contaminants deposited in the snow end up in the tundra and rivers at the end of winter. Furthermore, because the snow blankets virtually the entire Alaskan arctic region, this temporal record is widely available. This is an extremely attractive record if we can learn how to interpret it, particularly when we consider that there is only one first order atmospheric monitoring station in all of arctic Alaska. If snow can be established as a proxy for arctic haze and other atmospheric contaminants then snow chemistry can greatly add to our ability to delineate the spatial deposition of atmospheric contaminants in remote areas.

In the study reported here, we use sampling by layer to develop a temporal and spatial picture of aerosol loading to the snow pack of northwest Alaska. The sampling was done during a 1200 km snowmobile transect that took place in March and April, 2002, when snow depth and haze concentrations should have been at their maximum. The winter of 2001-2002 had historically above-average atmospheric haze concentrations (Fig. 2) so presumably aerosol concentrations in the snow were also above average. The goal of the work was to measure the spatial and temporal distribution of snow pack chemistry in northwestern Alaska, and to try and explain the observed patterns.

The traverse extended from Nome, on the Bering Sea, to Barrow, on the Beaufort Sea (Fig. 3). Air temperatures in Nome are substantially higher than in Barrow and the Bering Sea has a less extensive ice cover in winter than the Beaufort Sea (Gloersen et al., 1992; Parkinson and Gloersen, 1993) and it is ice-free in summer.

EXPERIMENTAL PROCEDURES

Stratigraphic Control and Sampling

Snow samples for major element analysis were collected at 16 sites spaced equally north and south of the Brooks Range between March 24 and April 26, 2002 (Figure 3 and Table 1). All sample sites were

located in flat, treeless areas away from villages, towns, roads, or trails in order to minimize potential contamination. Additional samples were collected for trace element analysis at five of the 16 sites. At each site, a snow pit was dug and samples were taken from the lower, middle, and top parts of the snow pack, with the samples keyed to strata that could be cross-correlated from one location to the next. The dates when these strata were deposited were determined from meteorological measurements and volunteer snow observations collected at seven villages and two automated weather stations (Fig. 1B) along the route. At each site layer density, hardness, thickness and grain characteristics served as the basis for cross correlation of snow layers.

To ensure that our activities did not result in contamination, samples were collected from snow pits dug hundreds of meters upwind from where we stopped our snowmobiles. Field personnel approached sampling sites on foot from the downwind direction. Major element samples were taken from pits excavated over tundra while trace element samples were obtained from pits located on frozen lakes. The frozen lake sites were selected to minimize potential contamination from underlying vegetation or soil. Tools for excavating and sampling snow were constructed of pre-cleaned polystyrene and were stored in pre-cleaned polyethylene bags. Shovels used to dig the snow pits were cleaned with HPLC grade hexane before and after sampling and were stored in pre-cleaned polyethylene bags during transportation. Layers were sampled from the base to the top of the snow pack to minimize potential cross contamination. Samples were placed immediately inside pre-cleaned plastic coolers for shipment and remained frozen during storage and shipping.

Trace elements

Prior to sampling, 500 mL wide-mouth polytetrafluoroethylene (PTFE Teflon) bottles and 100 mL scoops were cleaned following the methods of Bloom (1995) and were stored triple wrapped in pre-cleaned polyethylene bags. Snow sampling personnel wore full-body Tyvek suits, rubber boots, Tyvek hoods, surgical masks and two pairs of talc-free nitrile gloves. A different set of protective clothing was worn at each of the 5 sample locations. A “clean hands/dirty hands” technique similar to EPA Method

1669 (Bloom, 1995; Snyder-Conn et al., 1997) was used during collection of the trace element samples. Three Hg samples and three trace element samples were taken from each of the three target layers for a total of eighteen samples at each site. A separate pre-cleaned scoop was used to collect each set of triplicate samples from a layer.

Major elements, specific conductance and pH

Major element samples were collected in pre-cleaned tripled polypropylene bags by field personnel using pre-cleaned 200 cm³ polypropylene scoops while wearing talc free nitrile gloves. Duplicate samples were taken at three of the 16 sample locations and were analyzed for consistency. Laboratory analytical procedures, detection limits, and accuracy of repeated values for both trace and major elements are described in Appendix 1.

RESULTS

The Snow Pack of 2001-2002

Figure 4 shows the snow stratigraphy at the five sites where trace element samples were collected. Snow depths along the southern half of the transect were below average during the winter of 2001-2002 due to a late start of winter snowfall (Fig. 1B), but were average in the northern half of the transect. Above freezing temperatures, and even one rain-on-snow event, occurred during the winter, producing several ice layers and icy features in the snow. These features were pronounced at Council at the south end of the transect, but were almost invisible north of the Brooks Range, reflecting the gradient in temperature that extends over this region of Alaska. The melt layers, which could be dated precisely from meteorological records, provided a helpful time line and a check on our cross-correlation between sites (dashed lines in Fig. 4). We also used recorded periods of snow and wind to develop the time line. Our best interpretation suggests that the three layers of snow that were sampled should be assigned dates of late December, 2001, mid-January and mid-March, 2002.

Snow layers underwent three types of post-depositional metamorphism (Sturm, 2002). Near the south end of the transect melting and percolation of water in the snow probably mobilized some major and trace elements and moved them downward with the water. Only the stratigraphically lowest samples at the southernmost sites appear to have been affected by this type of metamorphism (Fig. 4). From Selawik (Fig. 3) north, stratigraphic evidence indicates little or no melting took place. Wind redistribution also occurred at selected sites, but our experience (Sturm et al., 2001) is that for the formation of a slab in the Arctic simultaneous wind and snow fall are usually required. These layers are therefore likely to have had a similar chemical signature to a layer deposited without wind. Lastly, depth hoar metamorphism affected many layers of snow. Little is known about how this temperature gradient driven process might mobilize chemical constituents, but for non-volatile chemicals the distance moved through the snow pack is likely to be limited.

Sulfate and Trace Elements in the Snow

Sulfur in the form of SO_4^{2-} is the predominant ion in arctic haze (Barrie, 1986; Brock et al., 1990; Shaw, 1995). Consequently, its concentration in the snow pack is likely to be most representative of the haze concentration. The primary sources of SO_4^{2-} are industrial and auto emissions while a second source is the rapid, irreversible, oxidation of SO_2 to SO_4^{2-} in the atmosphere (Jaeschke et al., 1999). Studies (Li et al., 1993; Jaffrezo et al., 1994) show that in the Arctic winter 75 to 85% of all SO_4^{2-} is of anthropogenic origin and since most of these sources are not in the Arctic this anthropogenic SO_4^{2-} has traveled long distances.

Many studies on the formation of arctic haze have shown that maximum aerosol concentrations in the lower atmosphere are found in the late-winter and early spring (Mitchell, 1956; Shaw, 1975; Rahn et al., 1977; Rahn, 1981; Barrie and Hoff, 1985; Barrie, 1986; Bodhaine, 1989; Cheng et al., 1993). Following Norman et al. (1999) we have plotted non-sea salt SO_4^{2-} concentrations as a measure of the SO_4^{2-} in the snow samples that was of non-marine origin (Fig. 5). These plots show a distinct late-winter increase at 13 of the 16 sample sites along the traverse route indicating lower concentrations of non-sea salt SO_4^{2-} in

the bottom two layers of snow (late December and mid-January) than in the top layer (mid-March). Based on the data from all 16 sites, non-sea salt SO_4^{2-} loading was significantly higher in the late winter snow pack at the 98% confidence level ($\text{Prob}>F=<0.0138$). Our results agree with the work of Polissar et al. (1998b) who found that maximum non-sea salt SO_4^{2-} aerosol concentrations in northwest Alaska occurred in late winter or early spring. Our results extend this finding, previously limited to coastal sites where aerosols were sampled, to a region 1200 km in extent.

Sulfate loading in the late winter snow pack was elevated throughout the range of Cl concentrations. This is supported by a conditional lattice analysis of non-sea salt SO_4^{2-} concentrations plotted over the four quartile ranges of Cl concentrations. High Cl concentrations are a good indicator of proximity to a marine source, yet across the entire spectrum of Cl values we measured in the snow pack the SO_4^{2-} concentrations remained elevated, suggesting its deposition was independent of the deposition of marine aerosols. In addition, as the winter progressed SO_4^{2-} became an increasingly larger component of the ionic pool: non-sea salt SO_4^{2-} accounted for 5% of the total ionic load in all December snow samples and 6% in January, but by March it was fully 13% of the total ionic load. This pattern is consistent with the pattern of seasonal increase in atmospheric haze concentration shown in Figure 1A.

Late-winter elevated values of arctic haze tracers Pb, Cd and As (Fig. 6 and Tables 2 and 3) parallel the temporal trend indicated SO_4^{2-} loading (Fig. 5). Among the suite of trace elements we measured, the best correlations were between Fe, V, Ni, Ba, and Pb ($r>0.7$ for all correlations). This suite of trace metals is commonly associated with anthropogenic aerosols (Xie et al., 1999), and the positive correlations are expected because these species come from the same sources and are likely to travel together (Snyder-Conn et al., 1997; Polissar et al., 1998b). Using Cd and Pb concentration values in an ANOVA, a late winter increase in concentration is supported at the 95% confidence level. The same trend is observed for As (Fig. 6) though at a lower level of significance. In general, dissolved concentrations of these trace elements were low but detectable. These generally low concentrations mirror published values showing that trace element loadings in both seasonal and perennial (i.e., the Greenland Ice Sheet) arctic snow

packs are low (Mart, 1983; Davidson et al., 1993; Barbante et al., 1997; Snyder-Conn et al., 1997; De Caritat et al., 1998; Gregurek et al., 1998; Sherrell et al., 2000; Garbarino et al., 2002; see also the table of published trace metal concentrations in melted snow samples included in Garbarino et al., 2002). These low loading concentrations arise primarily because the region is remote from most sources of anthropogenic contaminants.

Concentration values for SO_4^{2-} and trace elements were fairly homogeneous across the entire region (compare values from individual sites in Figs. 5 and 6), suggesting little or no regional trend in atmospheric concentration or scavenging efficiency. In addition, deposition was locally homogeneous at each site. Replicate samples within layers (error bars in Figure 6) showed surprisingly little scatter. With the notable exception of values from the middle snow layer (mid-January) sampled at the Brooks Range site, replicates generally fell within $\pm 15\%$ of each other. We interpret these results to indicate that the deposition of trace elements was both locally and regionally homogeneous with the only exception the site in the Brooks Range where exposed bedrock provided a local source for wind-blown dust.

In sharp contrast to the temporal and spatial patterns shown by non-sea salt- SO_4^{2-} and the trace elements, total Hg concentrations showed no significant change between early- and late-season snow at all sites except Atqasuk, the site closest to the Arctic Ocean Coast. No major terrain features exist between Atqasuk, at an elevation of 96 feet above sea level, and the Arctic Ocean. At Atqasuk, there was a monotonic increase in Hg with the middle (mid-January: 3.3 ± 1.5 ng/L) and top (mid-March: 6.2 ± 0.2 ng/L) snow layers showing progressively more elevated values in comparison to value for the basal layer of snow (Fig. 7). Hg increased with time only at sites close to the Arctic Coast. This pattern is reinforced by data from Barrow (Fig. 7 top panel, data from S. Brooks and S. Lindberg; see also Lindberg et al, 2002) where Hg concentrations in the snow are not only higher than at Atqasuk, but also increase through the winter. Lu et al. (2001), Snyder-Conn et al. (1997) and Garbarino et al. (2002) have also reported similar elevated

values of Hg at or near the Arctic Coast. In sharp contrast, at Council (elevation 85 feet above sea level), less than 30 km from the coast, little temporal signal and no coastal effect for Hg was observed.

Major elements, specific conductance and pH

The asymmetrical pattern for Hg in the snow was mirrored in the results for major elements, specific conductance and pH. Snow samples obtained within 50 km of the Arctic Ocean had elevated specific conductance values and high sea salt ion concentrations (Na and Cl), while samples obtained near the Bering Sea coast and far inland exhibited low values of both (Fig. 8: see also Table 3).

In contrast to the regional deposition patterns exhibited by SO_4^{2-} , trace elements and major ions, the presence of the Brooks Range could be identified in the pH results (Fig. 9). Coastal samples had pH values ranging between 4.7 and 5.5, but in the Brooks Range a ten-fold increase (to >6) was observed, a finding we attribute to the widespread exposure of carbonate rocks in the range (Mull et al., 1997). In addition, the Brooks Range typically experiences higher wind speeds and more exposed bedrock than the low-lying areas to the southwest and north. The seasonal trends in pH values were also asymmetric. In the Brooks Range and to the south there was little seasonal trend, with pH values from March similar to those from December (we exclude a single anomalous value from Council in the March snow layer). North of the Brooks Range the pH decreased monotonically throughout the winter.

DISCUSSION

The Snow Pack of 2001-2002

Trace element concentrations, particularly of Pb and Hg, were well below Environmental Protection Agency (EPA) contaminant levels in the snow pack of northwestern Alaska in 2002 (Figs. 6 and 7). The maximum contaminant level for Hg in drinking water is 2000 ng/L; the action level for Pb is 15,000 ng/L. The observed low values are consistent with other studies in the Arctic in which low trace element concentrations in snow have been reported (Mart, 1983; Davidson et al., 1993; Barbante et al., 1997;

Snyder-Conn et al., 1997; De Caritat et al., 1998; Gregurek et al., 1998; Sherrell et al., 2000; Garbarino et al., 2002).

Trace Elements, Sulfate and pH in the Snow

The trace elements in our snow samples (Table 2) were undoubtedly derived from arctic haze. Studies of haze composition (Shaw, 1995; Polissar et al., 1998b; Jaeschke et al., 1999) indicate the same suite of major and trace elements found in the snow pack. In most cases (i.e., for As, Cd, Pb, Hg, Ni, V) there are no local sources for these elements and measurements of atmospheric concentrations at Barrow and Resolute in Arctic Canada confirm their presence in haze in the North American sector of the Arctic (Davidson et al., 1989, 1993; Polissar et al., 1998b; Xie et al., 1999). Furthermore, by reporting non-sea salt SO_4^{2-} concentrations from melted snow samples filtered to less than $0.45 \mu\text{m}$ (Fig. 5), we have attempted to exclude the large diameter aerosol contributions not derived from haze. For these reasons we conclude that our measurements represent primarily haze constituents scavenged from the atmosphere during the winter. Because wet deposition is the most effective mode of aerosol scavenging (Bergin et al., 1995; Davidson et al., 1989; Uematsu et al., 2000), most of the elements were probably deposited contemporaneously with the snow. There were between 6 and 9 snow events during the winter along the 1200 km traverse route (Fig. 4), of which we sampled layers representing 4 to 5 events. We conclude that we captured about half of the total loading in the snow.

The characteristic increase in haze concentration through the winter (Fig. 1B) was mirrored by an increase in non-sea salt SO_4^{2-} (Fig. 5), Cd, Pb and As concentrations (Fig. 6) late in the winter. The coincidence of these two time series suggests that the snow layers may indeed provide a proxy of the winter haze concentration. It is a proxy, however, about which we have much to learn. A coordinated series of direct measurements of atmospheric haze along with careful, stratigraphically-controlled snow sampling is going to be needed to better understand how ionic concentrations measured in the snow relate to aerosol concentrations in the atmosphere. Because the snow pack is ubiquitous in the Arctic, such a

study would be worthwhile, potentially resulting in a snow sampling method that would allow extensive temporal and spatial representation of atmospheric conditions.

One key feature of the spatial distribution of SO_4^{2-} and trace elements is that the loading in the snow pack was basically uniform across northwestern Alaska. The Brooks Range, a formidable barrier to over-snow travel, proved to be no obstruction to arctic haze. Data from a network of aerosol sampling sites at Barrow and near Fairbanks in central Alaska show that periodic variations in haze concentration are nearly synchronous north and south of the range (Catherine Cahill, personal communication, 2002), confirming that the Brooks Range is not a barrier to haze.

Unlike the spatially uniform presence of Arctic haze elements (excluding Hg), the acidity of the snow showed a marked asymmetrical pattern (Fig. 9). The results suggest a pattern in which competing acidifying and buffering sources determine the local pH. For example, pH was constantly higher in the Brooks Range than anywhere else along the transect, a fact we attribute to the mechanical weathering of an extensive terrane of carbonate rocks found in this area (Mull et al., 1997).

Sulfate aerosol loading to the northwestern Alaskan Arctic

The results from this study can be used to estimate non-sea salt sulfate loading in northwestern Alaska. To make the estimate, we make some simplifying assumptions. First, the three layers we sampled constitute between 40 and 89% of the total snow pack at each site (Table 1; average of all sites is 60%). We assume the concentrations for these layers reflect the concentration of the entire snow pack. Second, we assume the mean snow water equivalent for the traverse, based on the bulk snow density ($\sim 300 \text{ kg/m}^3$) and the mean snow depth (0.5 m; see Table 1), was 150 kg/m^2 of water. Third, we compute the total non-sea salt SO_4^{2-} loading by multiplying the average concentration by the snow water equivalence. Because our concentration values are based on samples filtered to less than $0.45 \mu\text{m}$, we must account for non-sea salt SO_4^{2-} particles greater than $0.45 \mu\text{m}$. Based on data reported by Dibb and Jaffrezo (1997) and Tunved et al. (2003), we estimate that we lost about 40% by mass through the filtering process. We adjust upward for this loss. We also adjust the loading upward to account for the fact that only 70% of the total snow

pack had been deposited by the time we conducted our traverse (Fig. 1B; Council-50%; Brooks Range-90%). Lastly, we note winter is about 75% of the total year in our study area (9 out of 12 months). Combining all of these correction factors we estimate yearly non-sea salt SO_4^{2-} loadings to range from 12 to 281 $\text{mg/m}^2/\text{yr}$. This range is comparable to the non-sea salt SO_4^{2-} concentrations reported in surface snow and ice cores from Greenland by Mayewski et al., 1987.

Mercury in the 2001-2002 arctic Alaskan snow pack

Hg (Fig. 7), specific conductance, and Cl (Fig. 8) all exhibited an increase in concentration with increasing proximity to the Arctic Coast. Elevated Hg values extended inland more than 40 km and peaked at the Arctic Coast (Fig. 7). This pattern is consistent with measurements and theories suggesting that rapid deposition of Hg from the lower atmosphere to the snow pack occurs during Hg depletion events (MDEs; Schroeder et al., 1998; Lu et al., 2001; Lindberg et al., 2002). The MDEs require the presence of photochemically active halogen species (HOBr and HOCl) to oxidize gaseous elemental Hg (Hg^0) to reactive gaseous Hg (RGM; Hg^{2+}). These halogens come from a marine source, suggesting why there might be a peak in Hg, Cl and specific conductance at Barrow. More puzzling, however, is why there is no comparable increase in Hg or sea salts at or near the Bering Sea Coast.

The answer may lie in the availability of BrO and other halogens of marine origin and the trajectories that near-surface air masses follow in the two locations. We note that Hg in the Arctic winter atmosphere is present as gaseous elemental Hg (Hg^0). Hg^0 has a long residence time in the atmosphere (~1 year: Cheng and Schroeder, 2000) and travels widely. It is almost certainly uniformly distributed across northwest Alaska. It is deposited in the snow pack only when halogen radicals (Br and Cl) and halogen oxide radicals (BrO and ClO) are also present. The reactions are complex and photochemically driven. Recent studies have confirmed that deposition will not occur unless BrO levels are elevated (Lu et al., 2001; Lindberg et al., 2002). High BrO levels often coincide with periods of wind, wave activity, and formation of sea ice leads (Wagenbach et al., 1998).

The presence of salt aerosols (Na and Cl) of marine origin at Barrow and at the two sample sites south of Barrow (Fig. 8) suggests that BrO was also present at these locations during the winter. The low concentration of salt ions in snow samples across the remainder of the traverse route, and in particular, near the Bering Sea Coast at Council, suggests that at these locations the opposite was true. Since atmospheric Hg was undoubtedly present at all locations we think the absence of BrO explains the absence of Hg at the southern sample sites. The general absence of ions at the southern sites also supports the hypothesis they did not experience significant deposition of marine-derived aerosols.

The sample site at Council is actually closer to the ocean than the sample site at Atkasuk (Fig. 3: 30 km vs. 45 km), so why wasn't there any BrO at that location? The answer, we believe, lies in the direction of surface winds and storm tracks across the region. During the traverse, we recorded the direction of snow drift features (dunes, barchans, sastrugi: see Doumani, 1966) at 83 stations (Fig. 10). These measurements were taken in open, flat, treeless areas. Surface winds, of which sastrugi measurements are a proxy, should be within 15° of winds aloft (Wallace and Hobbs, 1977). The sastrugi measurements reveal regional patterns that we believe are representative of surface winds above the snow pack. Virtually all of these features indicated winds from the east or southeast for sites south of the Brooks Range. These winds came from an inland direction. At Barrow and to the immediate south, the winds came from the W or directly off the ocean. Winter climatologies and discussions with village residents along the routes confirm that the drift features were indicative of the main directions from which snowstorms arrived. U.S. weather service synoptic charts (K. Volz and P. Olsson, Alaska Experimental Forecast Facility, personal communication) indicate the same. As a consequence, the "effective distance from the coast" for Council and the sites near it was much greater than the straight line distance to the ocean. We have estimated what this effective distance was by comparing the curves for Cl concentration inland from the Bering Sea Coast to the curve inland from the Arctic Coast (Fig. 8). It is roughly 150 km. We note that marine salt aerosol concentrations were very low at this same distance inland from Barrow on the northern end of the traverse. Two additional points about BrO. The bulk of activity during BrO

driven MDEs occurs in the lowest 1 km of air above the ground surface. Additionally, BrO does not survive long in the atmosphere as it is rapidly broken down to Br⁻ compounds and oxygen gas in a time frame of a few hours (McConnell et al., 1992; Hausmann and Platt, 1994; Lindberg et al., 2002). Our sastrugi measurements are the closest proxy of wind directions below 1 km elevation during snow deposition and potential MDE driven Hg deposition. Even if BrO was initially present in Bering Sea air masses it would probably be heavily depleted after traveling ~150 km inland.

The concept of “effective distance from the coast” may help to explain some of the more puzzling aspects of known concentrations of Hg deposition in the North American Arctic snow pack. Hg concentrations in melted snow samples from 11 sites in northeastern arctic Alaska are presented by Snyder-Conn et al. (1997), values for 5 coastal sites in NW arctic Alaska are published by Garbarino et al. (2002) and data for Barrow is available from Lindberg et al. (2002). Lu et al. (2001) report values from 31 sites across arctic Canada. The data show that across all of arctic Alaska, where a low, flat plain extends inland from the coast, Hg levels in snow decline to the south but are still noticeably elevated as much as 50 km inland. Throughout this area one predominant storm wind direction is from the north and northwest, so winds bring halogens inland and facilitate Hg deposition to the snow pack. In Canada, most of the sites reported by Lu et al. (2002) are on the coast and, as expected, have relatively high (>50 ng/L) concentrations of Hg in the snow. However, there are at least 6 examples of coastal sample sites where Hg concentrations measured from snow samples are less than 10 ng/L. We do not know the particular meteorological details for each site, but perhaps at some of these locations storm tracks follow circuitous routes so that air masses arrive after passage over considerable stretches of land and are depleted in the halogens necessary for Hg deposition.

There is an alternative hypothesis that can account for the regional asymmetry in Hg deposition. The production of BrO and other halogens is higher in the Beaufort than in the Bering Sea. GOME satellite measurements have been used to “map” elevated BrO concentrations (Hausmann and Platt, 1994). These records indicate more prevalent and higher concentrations north of Alaska than west of it (Lu et al., 2001;

Lindberg et al., 2002). Perhaps wind and ice conditions in the Beaufort Sea favor the production of BrO in comparison with the Bering Sea.

Conclusions

Layer-based sampling allowed us to assemble a time record of loading from the layered snow pack across northwestern Alaska. This record indicated that concentrations of trace elements representative of arctic haze (Pb, Cd, Ni) were higher in the mid-March snow layer than in the late December or mid-January snow layers, a pattern that mimics the seasonal rise of atmospheric haze concentration (Fig. 1A). The issue of whether the loading is a useful proxy for atmospheric concentrations is, and probably will, remain an open question for some time, but the fact that a snow-layer based time evolution is in general agreement with the evolution of the aerosol concentration at Barrow suggests the method has potential.

The traverse route was bisected by the Brooks Range, a formidable east-west mountain range that we had initially hypothesized would limit the southward extent of haze. This proved not to be the case, with trace element concentrations similar in coeval snow layers throughout the traverse route. We show in another paper (Sturm and Liston, in press) that the Brooks Range was also not a barrier to snow storm tracks. We conclude that though a formidable barrier to snow mobile travel, the range, with a mean elevation less than 2100 m, poses little impediment to the movement of air masses.

Our most topical finding was that Hg was elevated only in samples close to and south of the Arctic Coast near Barrow, but was not elevated in comparable samples inland from the Bering Sea coast. Marine salts (Na, Cl) and non-sea salt SO_4^{2-} showed the same pattern. Taken together, these findings provide support for current theories (Schroeder et al., 1998; Lu et al., 2001; Lindberg et al., 2002) that Hg in the snow is a result of a combination of complex photochemical reactions that require a halogen source associated with marine air. Near Barrow, surface winds and prevailing storm tracks carry BrO directly and rapidly inland, producing the necessary components for Hg depletion and deposition. In contrast, winds and storms along the southern part of the sampling route come from inland and are likely depleted in BrO. We capture this difference by computing the “effective distance from the coast” for both

locations. South of Barrow (Atqasuk) this distance is equal to the straight-line distance to the ocean (~40 km) but for the sites inland from the Bering Sea it is about 150 km.

ACKNOWLEDGMENTS

This work benefited from discussions with G. Shaw, E. Snyder-Conn, W. Simpson, C. Cahill, D. Perovich, K. Volz, P. Olsson and T. Brabets. Discussions with Steve Brooks and Steve Lindberg helped to codify the Hg story. The manuscript was improved by the suggestions of D. Hawkins and M. Poage and two anonymous referees. This project was funded by the National Science Foundation Office of Polar Programs (OPP-9732077) with supplemental funding from the Atmospheric Sciences Program. G. Liston, A. Chevront, and K. Tape deserve special recognition for collecting samples in extremely cold conditions. J. Holmgren and E. Pyne assisted in the field. N. Bloom and E. Prestbo of Frontier Geosciences performed trace element analyses while P. Zeitz at Dartmouth College provided major ion analyses. A. Jefferson and J. Ogren of the NOAA Climate Monitoring and Diagnostics Laboratory provided arctic haze data from Barrow. High school students in Buckland, Selawik, Ambler, Atqasuk, and White Mountain, Alaska provided meteorological measurements.

REFERENCES

- AMAP, 1997. "Arctic Pollution Issues: A State of the Arctic Environment Report." Arctic Monitoring and Assessment Programme, P.O. Box 8100 Dep., N-0032 Oslo, Norway, 188 pp.
- Barbante, C., Bellomi, T., Mezzadri, G., Cescon, P., Scarponi, G., Morel, C., Jay, S., Van De Velde, K., Ferrari, C., and Boutron, C.F., 1997. Direct determination of heavy metals at picogram per gram levels in Greenland and Antarctic snow by double focusing inductively coupled plasma mass spectrometry. *Journal of Analytical Atomic Spectrometry* 12, 925-931.
- Barrie, L.A. and Hoff, R.M., 1985. Five years of air chemistry observation in the Canadian Arctic, *Atmospheric Environment* 20 1995-2010.
- Barrie, L.A., 1986. Arctic air pollution: An overview of current knowledge. *Atmospheric Environment* 20 643-663.
- Bergin, M.H., Jaffrezo, J.-L., Davidson, C.I., Dibb, J.E., Pandis, S.N., Hillamo, R., Maenhaut, W., Kuhns, H.D., and Makela, T., 1995. The contributions of snow, fog, and dry deposition to the summer flux of anions and cations at Summit, Greenland. *Journal of Geophysical Research* 100(D8) 16,275-16,288.
- Bloom, N. S., 1995. Mercury as a case study of ultra-clean sample handling and storage in aquatic trace metal research. *Environmental Lab* 3-4, 20-25.
- Bloom, N.S and Fitzgerald, W.F., 1988. Determination of Volatile Mercury Species at the Picogram Level by Low Temperature Gas Chromatography With Cold Vapor Atomic Fluorescence Detection. *Analytica Chimica Acta* 208 151-161.
- Bloom, N.S and Crecelius, E.A., 1983. Determination of Mercury in Seawater at Sub-Nanogram per Liter Levels. *Marine Chemistry* 14 49-59.
- Bodhaine, B.A., 1989. Barrow surface aerosol: 1976-1986. *Atmospheric Environment* 11, 2357-2369.
- Bodhaine, B. A., Dutton, E.G., DeLuisi, J.J., Herbert, G.A., Shaw, G.E., and Hansen, A.D.A., 1989. Surface aerosol measurements at Barrow during AGASP II, *Journal of Atmospheric Chemistry* 9 213-224.
- Brock, C.A., Radke, L.F., P.V. Hobbs, P.V., 1990. Sulfur in particles in arctic hazes derived from airborne in situ and lidar measurements. *Journal of Geophysical Research* 95, 22,369-22,387.
- Cheng, M.-D., Hopke, P.K., Barrie, L., A., Rippe, A., Olson, M., and Landsberger, S., 1993. Qualitative determination of source regions of aerosol in Canadian High arctic. *Environmental Science and Technology* 27, 2063-2071.
- Cheng, M.-D., and Schroeder, W.H., 2000. Potential atmospheric transport pathways for mercury measured in the Canadian high arctic. *Journal of Atmospheric Chemistry* 35, 101-107.
- Crecelius, E.A; Bloom, N.S; Cowan, C.E. and Jenne, E.A., 1986. Speciation of Selenium and Arsenic in Natural Waters and Sediments, Volume 2: Arsenic Speciation. Final Report Prepared for Electric Power Research Institute, Palo Alto, CA by Battelle Pacific Northwest Laboratories, Richland Washington.

- Davidson, C.I., Harrington, J.R., Stephenson, M.J., Small, M.J., Boscoe, F.P., and Gandley, R.E., 1989. Seasonal variations in sulfate, nitrate and chloride in the Greenland ice sheet: relationship to atmospheric concentrations. *Atmospheric Environment* 23(11) 2483-2493.
- Davidson, C.I., Jaffrezo, J.-L., Mosher, B.W., Dibb, J.E., Borys, R.D., Bodhaine, B.A., Rasmussen, R.A., Boutron, C.F., Gorlack, U., Cachier, U., Ducret, J., Colin, J.-L., Heidam, N.Z., Kemp, K., and Hillamo, R., 1993. Chemical constituents in the air and snow at DYE 3, Greenland: I. Seasonal variations. *Atmospheric Environment* 27A, 2709-2722.
- De Caritat, P., Åyrås, Niskavaara, H, Chekushin, V., Bogatyrev, I, and Reimann, C., 1998. Snow composition in eight catchments in the Central Barents Euro-Arctic Region. *Atmospheric Environment* 32, 2609-2626.
- Delene, D.J., and Ogren, J.A., 2002. Variability of aerosol optical properties at four North American surface monitoring sites. *Journal of Atmospheric Sciences* 59(6) 1135-1150.
- Dibb, J.E., and Jaffrezo, J.-L., 1997. Air-snow exchange investigations at Summit, Greenland: An overview. *Journal of Geophysical Research* 102(C12), 26,795-26,807.
- Dominé, F., and Shepson, P.B., 2002. Air-snow interactions and atmospheric chemistry. *Science* 297 1506-1510.
- Doumani, G. A., 1966. Surface Structures in Snow. In: International Conference on Low Temperature Science, Sapporo, Japan, Aug.14-19, 1966, Proceedings, Publisher: Sapporo, Institute of Low Temperature Science, Hokkaido University, Japan Vol.1, Part 2, p.1119-1136.
- Garbarino, J.R., Snyder-Conn, E., Leiker, T.J. and Hoffman, G.L., 2002. Contaminants in Arctic snow collected over sea ice. *Water, Air and Soil Pollution* 139 183-214.
- Gloersen, P., Campbell, W.J., Cavalieri, D.J., Comiso, J.C., Parkinson, C.L. and Zwally, H.J., 1992. Arctic and Antarctic sea ice, 1978-1987: Satellite passive-microwave observations and analysis, NASA SP-511, NASA, Washington D.C. 290 p.
- Gregurek, D., Reimann, C., and Stumpfl, E.F., 1998. Trace elements and precious metals in snow samples from the immediate vicinity of Nickel processing plants, Kola Peninsula, Northwest Russia. *Environmental Pollution* 102, 221-232.
- Hausmann, M., and Platt, U., 1994. Spectroscopic measurement of bromine oxide and ozone in the high Arctic during Polar Sunrise Experiment 1992. *Journal of Geophysical Research* 99(D12), 25,399-25,413.
- Herbert, G. A., Harris, J. M. and Bodhaine, B. A., 1989. Atmospheric transport during AGASP-II: The Alaskan flights (2-10 April 1986), *Atmospheric Environment* 23 2521-2536.
- Jaffrezo, J.-L., Davidson, C.I., Legrand, M. and Dibb, J.E., 1994. Sulfate and MSA in the air and snow on the Greenland Ice Sheet. *Journal of Geophysical Research* 99(D1) 1241-1253.
- Jaeschke, W., Salkowski, T., Dierssen, J.P., Trümbach, J.V., Krischke, U., and Günther, A., 1999. Measurements of trace substances in the Arctic troposphere as potential precursors and constituents of arctic haze. *Journal of Atmospheric Chemistry* 34, 291-319.

- Li, S.M., R.W. Talbot, L.A. Barrie, R.C. Harriss, C.I. Davidson, and J.L. Jaffrezo, 1993. Seasonal and Geographic Variations of Methanesulfonic Acid in the Arctic Atmosphere. *Atmospheric Environment* 27A 3011-3024.
- Lindberg, S.E., Brooks, S., Lin, C.-J., Scott, K.J., Landis, M.S., Stevens, R.K., Goodsite, M., and Richter, A., 2002. Dynamic oxidation of gaseous mercury in the Arctic troposphere at Polar sunrise. *Environmental Science and Technology* 36, 1245-1256.
- Lu, J.Y., Schroeder, W.H., Barrie, L.A., Steffen, A., Welch, H.E., Martin, K., Lockhart, L., Hunt, R.V., Boila, G., and Richter, A., 2001. Magnification of atmospheric mercury deposition to polar regions in springtime: the link to tropospheric ozone depletion chemistry. *Geoph. Res. Lett.*, 28(17), 3219-3222.
- Mart, L., 1983. Seasonal variations of Cd, Pb, Cu and Ni levels in snow from the eastern Arctic Ocean. *Tellus* 35B, 131-141.
- Mayewski, P.A., Spencer, M.J., Lyons, W.B., and Twickler, M.S., 1987. Seasonal and spatial trends in South Greenland snow chemistry. *Atmospheric Environment* 21(4) 863-869.
- McConnell, J.C., Henderson, G.S., Barrie, L., Bottenheim, J., Niki, H., Langford, C.H. and Templeton, E.M.J., 1992. Photochemical bromine production implicated in arctic boundary-layer ozone depletion. *Nature*, 355, 150-152.
- Mitchell, J.M., Jr., 1956. Visual range in the polar regions with particular reference to the Alaskan Arctic. *Journal of Atmospheric and Terrestrial Physics*. 195-211.
- Mull, C.G., Harris, A.G., and Carter, J.L., 1997. Lower Mississippian (Kinderhookian) biostratigraphy and lithostratigraphy of the western Endicott Mountains, Brooks Range, Alaska. *Geologic Studies in Alaska by the United States Geological Survey* edited by J. A. Dumoulin and J. E. Gray, U.S. Geological Survey Professional Paper 1574, 328 p.
- Norman, A.L., Barrie, L.A., Toom-Sauntry, D., Sirois, A., Krouse, H.R., Li, S.M., and Sharma, S., 1999. Sources of aerosol sulphate at Alert: Apportionment using stable isotopes. *Journal of Geophysical Research* 104(D9), 11,619-11,631.
- Oehme, M., and Ottar, B., 1984. The long range transport of polychlorinated hydrocarbons to the Arctic. *Geophysical Research Letters* 1133-1136.
- Parkinson, C.L. and Gloersen, P., 1993. Global sea ice coverage. In: Gurney, R.J., Foster, J.L., and Parkinson, C.L., eds., *Atlas of satellite observations related to climate change*, p. 371-383.
- Polissar, A.V., Hopke, P.K., Paatero, P., Malm, W.C., and Sisler, J.F., 1998a. Atmospheric aerosol over Alaska 1. Spatial and seasonal variability. *Journal of Geophysical Research* 103(D15) 19,035-19,044.
- Polissar, A.V., Hopke, P.K., Malm, W.C., and Sisler, J.F., 1998b. Atmospheric aerosol over Alaska 2. Elemental composition and sources. *Journal of Geophysical Research* 103(D15) 19,045-19,057.
- Polissar, A.V., Hopke, P.K., Paatero, P., Kaufmann, Y.J., Hall, D.K., Bodhaine, B.A., Dutton, E.G. and Harris, J.M., 1999. The aerosol at Barrow, Alaska: long-term trends and source locations. *Atmospheric Environment* 33, 2441-2458.

- Polissar, A.V., Hopke, P.K., and Harris, J.M., 2001. Source regions for atmospheric aerosol measured at Barrow, Alaska. *Environmental Science and Technology* 35, 4214-4226.
- Rahn, K.A., Borys, R.D., and Shaw, G.E., 1977. The Asian source of arctic haze clouds. *Nature* 268, 713-715.
- Rahn, K.A., 1981. Relative Mn/V ratio as a tracer of large-scale tracers of pollution aerosol for the Arctic. *Atmospheric Environment* 15, 1457-1464.
- Schroeder, W.H., Anlauf, K.G., Barrie, L.A., Li, J.Y., Steffen, A., Schneeberger, D.R., and Berg, T., 1998. Arctic springtime depletion of mercury. *Nature*, 394, 331-332.
- Shaw, G.E., 1975. The vertical distribution of atmospheric aerosols at Barrow, Alaska. *Tellus* 27, 39-50.
- Shaw, G.E., 1995. The Arctic haze phenomenon. *Bull. Amer. Met. Soc.* 76(12), 2403-2413.
- Sherrell, R.M., Boyle, E.A., Falkner, K.K., and Harris, N.R., 2000. Temporal variability of Cd, Pb and Pb isotope deposition in central Greenland snow. *Geochemistry, Geophysics, Geosystems* 1, paper number 1999GC000007, 27 pp.
- Snyder-Conn, E., Garbarino, J.R., Hoffman, G.L., and Oelkers, A., 1997. Soluble Trace Elements and Total Mercury in Arctic Alaskan Snow. *Arctic*, 50, 201-215.
- Sturm, M. Liston, G.E., Benson, C.S., and Holmgren, J., 2001. Characteristics and growth of a snowdrift in arctic Alaska, U.S.A. *Arctic, Antarctic, Alpine Res.* 33(3) 319-329.
- Sturm, M. and Liston, G. E. (in press) The snow cover on lakes of the Arctic Coastal Plain of Alaska, U.S.A., *Journal of Glaciology*.
- Sturm, M., 2002. Snow. *The Encyclopedia of Atmospheric Sciences*, Academic Press, p. 2061-2072.
- Tunved, P., Hansson, H.C., Kulmala, M. Aalto, P. Viisanen, Y. Karlsson, H. Kristensson, A. Swietlicki, E. Dal Maso, M. Ström, J. and Komppula., M., 2003. One year boundary layer aerosol size distribution data from five Nordic background stations. *Atmospheric Chemistry and Physics Discussions* 3, 2783-2833.
- Uematsu, M., Kinoshita, K., and Nijiri, Y., 2000. Scavenging of insoluble particles from the marine atmosphere over the sub-Arctic North Pacific. *J. Atmos. Chem.*, 35 151-164.
- Wagenbach, D., Ducroz, F., Mulvaney, R., Keck, L., Minikin, A., Legrand, M., Hall, J.S., and Wolff, E.W., 1998. Sea-salt aerosol in coastal Antarctic regions, *Journal of Geophysical Research* 103 (D9), 10,961-10,974, 1998.
- Wallace, J.M., and Hobbs, P.V., 1977. *Atmospheric Science, an Introductory Survey*. Academic Press, New York, 467 pp.
- Xie, Y.-L., Hopke, P.K., Paatero, P., Barrie, L.A., and Li, S.-M., 1999. Identification of source nature and seasonal variations of Arctic aerosol by positive matrix factorization. *Journal of Atmospheric Sciences* 56(2), 249-260.

Table captions

Table 1. Sample names, locations, types and snow pack thickness for this study.

Table 2. Trace element concentrations $\pm 1\sigma$ (n=3) from this study. The < indicates the concentration was below the method detection limit given

Table 3. Major element concentrations, pH and specific conductance measured in snow melt samples collected during this study. IC=Ion chromatography; ICP-OES= inductively coupled plasma optical emission spectroscopy.

Figure captions

Figure 1A. Seasonal increase in haze concentration (as measured by light transmission) at Barrow, Alaska (data courtesy of the National Aeronautics and Atmospheric Administration's Climate Monitoring and Diagnostic Laboratory). The parameter plotted for arctic haze is atmospheric aerosol light scattering coefficient at 550 nm (1/Mm), an optical measure of the total atmospheric haze concentration (Delene and Ogren, 2002). Error bars indicate $\pm 1\sigma$ of the values measured for a given month between 1977 and 2002.

Figure 1B. Snow pack depths during the winter of 2001-2002 at Council (southern end of transect) and the Brooks Range. Arrows indicate the approximate dates of deposition for the snow layers that were sampled.

Figure 2. April arctic haze concentrations (atmospheric aerosol light scattering coefficient at 550 nm (1/Mm) at Barrow, Alaska. Error bars indicate $\pm 1\sigma$ of the average April monthly values from 1976-2002. Slightly above average concentrations are evident in April, 2002, the year and month of the traverse (data courtesy of NOAA-CMDL). The dashed line is the overall average of 11.7 from 1976 to 2002.

Figure 3. Traverse route from Nome to Barrow showing the sampling sites. Samples for major elements were collected at 16 sites. At 5 of these sites (solid black circles) samples for trace elements were also collected.

Figure 4. Snow stratigraphy at the five sites where trace element samples were obtained. The symbols denote the type of snow in each layer. Dashed lines indicate the correlation of layers between sites. Heavy brackets indicate layers that were sampled for trace and major elements.

Figure 5. Non-sea salt SO_4^{2-} concentrations at 16 sites between Nome and Barrow, Alaska, showing the increase in concentration late in the winter. Observed values ranged from 0 to 1695 $\mu\text{grams/Liter}$. Two different vertical axis scales are used in order to highlight the seasonal trend.

Figure 6. Trace element concentrations of Cd, Pb and As between Council and Barrow showing an increase in concentration late in the winter. The error bars represent the variability in the concentrations found in the three subsamples from each snow layer.

Figure 7. Concentrations of Hg between Council and Barrow for three layers of snow that fell in late December, mid-January and mid-March. 2000 data for Barrow (stars) are from Lindberg et al., 2002; 2002 data for Barrow (diamonds) are from S. Brooks and S. Lindberg (personal communication).

Figure 8. Cl concentrations in snow layer as a function of distance from the nearest coast. The average for all 3 layers of snow is plotted. Na shows a similar pattern. The arrow indicates a 150 km offset, which would be the “effective distance to the coast” at Council. Note that if the data for the sample sites nearest the Bering Sea coast are shifted to the right, they match the data for the Arctic Coast when offset inland ~150 km.

Figure 9. pH of melted snow collected between Council and Barrow showing markedly higher values in the Brooks Range, a strong seasonal trend north of the range, and little seasonal trend within or south of the range. The gray boxes, open circles and black triangles represent the dates of the three snow layers that were sampled (late December, 2001, mid-January and mid-March, 2002, respectively).

Figure 10. Map of northwestern Alaska with the locations and directions of sastrugi measured along the sampling transect. The tails of the arrows indicate the sample location.

Table 1. Sample names, locations and types and snow pack thickness for this study

Sample site	Latitude (°N)	Longitude (°W)	Date sampled	Sample type obtained	Snow pack thickness (cm)	Total thickness of layers sampled (cm)	% of total snow pack sampled
Council	64.849	163.649	24-Mar	Major and trace	56	41	73
CB-1T	65.034	163.291	26-Mar	Major	46	25	54
CB-3T	65.191	162.273	27-Mar	Major	50	28	56
CB-4T	65.327	162.005	28-Mar	Major	49	28	57
CB-8T	65.855	161.42	30-Mar	Major	25	19	76
BS-3T	66.355	160.568	1-Apr	Major	40	30	75
Selawik	66.703	158.716	5-Apr	Major and trace	68	43	63
SA-6T	67.014	157.918	7-Apr	Major	55	49	89
AI-3	67.465	157.6	9-Apr	Major	66	45	68
Brooks Range	68.126	156.347	11-Apr	Major and trace	33	24	73
ICO-4	68.24	155.575	15-Apr	Major	67	27	40
Colville	69.017	155.568	16-Apr	Major and trace	76	39	51
CO-11	69.498	155.606	19-Apr	Major	58	32	55
OA-10	70.193	156.648	21-Apr	Major	40	17	43
Atqasuk	70.698	157.309	23-Apr	Major and trace	58	29	50
Barrow	71.326	156.619	26-Apr	Major	33	21	64

Table 2. Trace element concentrations $\pm 1\sigma$ (n=3) from this study. < indicates the concentration was below the method detection limit

Measurement method		Al ($\mu\text{g/L}$)	As (ng/L)	Ba (ng/L)	Cd (ng/L)	Pb (ng/L)	Fe ($\mu\text{g/L}$)	Mn (ng/L)
Method detection limit		1.7	7.7	19	0.4	2	1.3	4
Site	Deposition date							
Council	Mid-March	53 \pm 27	86 \pm 10	690 \pm 290	19 \pm 6.1	596 \pm 114	33 \pm 17	1260 \pm 550
Council	Mid-January	11 \pm 2	12 \pm 4	176 \pm 20	2 \pm 0.8	55 \pm 8	6 \pm 1	220 \pm 50
Council	Late December	77 \pm 3	34 \pm 8	1200 \pm 80	3 \pm 0.4	92 \pm 5	63 \pm 2	1400 \pm 32
Selawik	Mid-March	268 \pm 18	126 \pm 30	4780 \pm 300	10 \pm 0.9	319 \pm 3	197 \pm 12	5420 \pm 330
Selawik	Mid-January	442 \pm 38	188 \pm 10	8740 \pm 830	13 \pm 0.4	353 \pm 48	273 \pm 21	8680 \pm 620
Selawik	Late December	113 \pm 10	123 \pm 30	2390 \pm 410	6 \pm 2.8	175 \pm 17	184 \pm 17	3460 \pm 420
BrooksRange	Mid-March	314 \pm 109	80 \pm 10	3600 \pm 90	9 \pm 0.9	468 \pm 28	181 \pm 27	9200 \pm 3270
BrooksRange	Mid-January	294 \pm 317	56 \pm 50	2820 \pm 2780	8 \pm 6.8	328 \pm 235	168 \pm 176	7090 \pm 6700
BrooksRange	Late December	92 \pm 44	13 \pm 4	760 \pm 310	2 \pm 1.2	82 \pm 36	62 \pm 30	2800 \pm 1310
Colville	Mid-March	155 \pm 17	57 \pm 3	4780 \pm 1300	6 \pm 0.9	262 \pm 12	99 \pm 7	2700 \pm 260
Colville	Mid-January	14 \pm 2	14 \pm 2	261 \pm 100	0.3 \pm 2.0	70 \pm 6	8 \pm 1	240 \pm 36
Colville	Late December	8 \pm 2	9 \pm 7	190 \pm 80	1 \pm 0.3	32 \pm 6	4 \pm 1	185 \pm 110
Atqasuk	Mid-March	158 \pm 5	110 \pm 30	2968 \pm 130	12 \pm 0.7	507 \pm 30	93 \pm 4	3320 \pm 340
Atqasuk	Mid-January	2w \pm 9	15 \pm 2	1981 \pm 1050	2 \pm 0.9	64 \pm 15	82 \pm 77	7470 \pm 2900
Atqasuk	Late December	147 \pm 8	93 \pm 10	3032 \pm 400	9 \pm 1.3	325 \pm 33	91 \pm 9	2760 \pm 270

Measurement method		Hg (ng/L)	Ni (ng/L)	Sr (ng/L)	U (ng/L)	V (ng/L)	Zn (ng/L)
Method detection limit		0.19	72	12	0.05	2.8	47
Site	Deposition date						
Council	Mid-March	1.4 \pm 0.2	110 \pm 20	500 \pm 100	2.6 \pm 1.1	130 \pm 50	750 \pm 140
Council	Mid-January	1.2 \pm 0.2	<72	380 \pm 30	0.8 \pm 0.1	25 \pm 4	670 \pm 270
Council	Late December	1.0 \pm 0.1	100 \pm 6	1200 \pm 310	8.2 \pm 3.5	200 \pm 6	2140 \pm 2050
Selawik	Mid-March	1.4 \pm 0.5	400 \pm 30	1200 \pm 20	14.0 \pm 0.3	640 \pm 40	1260 \pm 150
Selawik	Mid-January	1.3 \pm 0.0	620 \pm 30	1400 \pm 121	17.7 \pm 2.9	1060 \pm 80	1710 \pm 60
Selawik	Late December	1.7 \pm 0.5	340 \pm 100	2900 \pm 530	8.8 \pm 1.2	340 \pm 40	3170 \pm 2060
BrooksRange	Mid-March	1.7 \pm 0.1	310 \pm 70	1420 \pm 60	14.6 \pm 1.0	510 \pm 130	1050 \pm 190
BrooksRange	Mid-January	1.1 \pm 0.2	270 \pm 280	940 \pm 840	16.3 \pm 17.8	580 \pm 600	1100 \pm 750
BrooksRange	Late December	1.0 \pm 0.5	90 \pm 80	560 \pm 90	3.6 \pm 1.7	190 \pm 100	480 \pm 110
Colville	Mid-March	1.1 \pm 0.7	180 \pm 60	500 \pm 70	5.8 \pm 1.4	350 \pm 30	900 \pm 110
Colville	Mid-January	0.5 \pm 0.2	<72	100 \pm 20	0.7 \pm 0.1	25 \pm 4	130 \pm 60
Colville	Late December	0.8 \pm 0.5	<72	90 \pm 20	0.3 \pm 0.1	10 \pm 3	120 \pm 30
Atqasuk	Mid-March	6.2 \pm 0.2	200 \pm 20	7270 \pm 420	10.3 \pm 0.5	350 \pm 20	1400 \pm 240
Atqasuk	Mid-January	3.3 \pm 1.5	80 \pm 50	840 \pm 280	1.0 \pm 0.4	38 \pm 20	4000 \pm 1320

Table 3. Major element concentrations, pH and specific conductance measured in snow melt samples collected during this study. IC=Ion chromatography; ICP-OES= inductively coupled plasma optical emission spectroscopy.

		Cl ($\mu\text{g/L}$)	SO ₄ ²⁻ ($\mu\text{g/L}$)	Ca ($\mu\text{g/L}$)	K ($\mu\text{g/L}$)	Mg ($\mu\text{g/L}$)	Na ($\mu\text{g/L}$)	pH	Sp. Cond. ($\mu\text{S/cm}$)
Measurement method		IC	IC	ICP-OES	ICP-OES	ICP-OES	ICP-OES		
Method detection limit		5	16	20	100	70	30	0.1	0.1
Site Name	Deposition date								
Council	Mid-March	349	1790	110	<100	<70	360	4.5	13.3
Council	Mid-January	1212	250	110	<100	110	850	5.5	6.3
Council	Late December	354	130	110	<100	<70	310	5.5	3.6
CB-01T	Mid-March	1120	800	60	<100	120	770	4.9	9.7
CB-01T	Mid-January	300	90	60	<100	<70	320	5.5	2.6
CB-01T	Late December	402	160	140	300	<70	360	4.9	5.6
CB-03T	Mid-March	43	120	100	<100	<70	160	5.4	2
CB-03T	Mid-January	374	120	60	<100	<70	370	5.5	3
CB-03T	Late December	1335	330	60	120	140	870	5.3	7.3
CB-04T	Mid-March	254	310	120	<100	<70	270	5.1	4.2
CB-04T	Mid-January	205	60	90	<100	<70	250	5.4	2.5
CB-04T	Late December	265	120	110	100	<70	280	5.3	3.3
CB-08T	Mid-March	697	320	140	<100	90	500	5	6.4
CB-08T	Mid-January	529	190	140	<100	<70	410	5.3	4.2
CB-08T	Late December	698	150	170	150	100	450	5.1	5.5
BS-03T	Mid-March	507	200	120	<100	<70	390	5.2	4
BS-03T	Mid-January	555	190	130	<100	<70	410	5.3	3.9
BS-03T	Late December	563	160	120	<100	<70	450	5.4	4
Selawik	Mid-March	156	190	220	120	<70	210	5.6	2.4
Selawik	Mid-January	305	110	170	<100	<70	290	5.5	3
Selawik	Late December	126	110	2470	<100	110	200	5.3	3.3
SA-06T	Mid-March	177	100	160	<100	<70	230	5.6	2
SA-06T	Mid-January	228	140	240	<100	<70	250	5.6	2.7
SA-06T	Late December	51	60	160	<100	<70	160	5.7	1.5
AI-03	Mid-March	119	550	430	<100	110	200	6.2	4
AI-03	Mid-January	120	130	220	<100	<70	200	5.8	1.9
AI-03	Late December	127	160	410	<100	<70	210	6.1	3
Brooks Range	Mid-March	115	180	280	<100	<70	190	5.8	2.3
Brooks Range	Mid-January	323	110	120	<100	<70	300	5.3	3.3
Brooks Range	Late December	94	70	330	<100	190	220	6.3	3.5
ICO-04	Mid-March	262	160	100	<100	<70	260	5.2	4
ICO-04	Mid-January	17	30	90	<100	<70	150	5.3	2
ICO-04	Late December	22	40	90	<100	<70	140	5.3	2.2
Colville	Mid-March	251	140	110	<100	<70	240	5	5
Colville	Mid-January	176	80	100	<100	<70	210	5.2	3.2
Colville	Late December	23	60	110	<100	<70	140	5.6	1.4
CO-011	Mid-March	324	150	110	<100	<70	290	5	5
CO-011	Mid-January	530	120	100	<100	<70	440	5.2	4.8
CO-011	Late December	40	50	130	140	<70	1560	5.4	2
OA-10	Mid-March	2382	410	200	<100	190	1320	5.1	11.5
OA-10	Mid-January	1700	220	170	<100	140	960	5.2	8.2
OA-10	Late December	2702	150	1120	120	560	1250	6.8	14.5
Atqasuk	Mid-March	3863	560	270	140	360	1720	4.7	17.6
Atqasuk	Mid-January	6951	530	250	210	480	3430	5.3	23.7
Atqasuk	Late December	325	60	100	150	<70	330	5.4	3.4
Barrow	Mid-March	604	230	240	<100	70	430	4.7	4.3
Barrow	Mid-January	17880	1160	620	600	1760	2730	5.3	88.8
Barrow	Late December	11353	1000	420	320	840	5840	5.5	42.6

Appendix 1. Laboratory analytical procedures, detection limits and accuracy.

Trace elements

Trace element samples were prepared and analyzed under a Class-100 environment at Frontier Geosciences in Seattle, Washington. Triplicate sets of snow samples were acidified for preservation by the addition of 1.0 mL of trace-element grade HNO_3 , were allowed to thaw and then were thoroughly shaken and stored at room temperature until analysis. 100 ± 0.5 grams of each preserved sample was weighed into a specially cleaned wide-mouth 120 mL Teflon jar and placed on a Teflon-coated hotplate. 0.1 mL of concentrated trace-element grade 48 N HF was added to each sample and samples were reduced to less than 5 mL of total volume by sub-boiling evaporation at 90-100°C. After evaporation, the samples were diluted to 10.0 mL in HF/ HNO_3 cleaned polyethylene sample tubes, thus effecting a 10x concentration factor and dissolution of mineral particles. Eight 100 mL aliquots of milli-Q water containing 1% HNO_3 and 0.1% HF were similarly evaporated with the samples to generate method blanks. Samples were analyzed using a Perkin-Elmer Elan-6100 ICP-MS (inductively coupled plasma mass spectrometer). The estimated method detection limits for each analyte were calculated as three times the standard deviation of the eight blanks. Mean relative percent difference values calculated for all trace element concentrations measured in one set of duplicate samples were 20.0 or less, suggesting acceptable analytical precision. Analyses of eight sample blanks yield method detection limits in the low ng/L range for all elements.

Inorganic arsenic was measured from 10 mL aliquots of the original HNO_3 preserved samples prior to evapoconcentration. Samples were acidified with 1.0 mL of concentrated HCl and the arsenic hydrides were generated by manual injection of NaBH_4 below the solution surface with a syringe following the methods of Crecelius et al. (1986). The hydrides were transported by the argon carrier gas to a cryogenic trapping Gas Chromatographic (GC) column. After collection, the GC column was rapidly warmed to 180°C and the arsines were transported to a hydrogen/oxygen flame where As was determined by atomic absorption spectrometry (AAS). Only inorganic arsenic was detected. The mean relative percent

difference calculated for As concentrations measured in three sets of duplicate samples was 18.7 .

Analyses of eight sample blanks yield a method detection limit for As of 7.7 ng/L.

Mercury

Replicate sets of Hg samples were acidified by the addition of 1.0 mL of low Hg 0.2N BrCl in 12N HCl and the samples were allowed to thaw completely following the methods of Bloom and Creelius (1983). 50 mL aliquots of the BrCl oxidized samples were pre-reduced with NH_2OH to eliminate free halogens and then with SnCl_2 to reduce Hg(II) to Hg^0 . The Hg^0 was driven from solution by purging with N_2 , and was recollected on a gold-coated sand trap. The Hg was thermally desorbed from the gold trap to an Ar gas carrier and into the atom cell of a cold vapor atomic fluorescence spectrometer (Bloom and Fitzgerald, 1988). The mean relative percent difference calculated for Hg concentrations measured in five sets of duplicate samples was 1.4. Analyses of eight sample blanks yield a method detection limit for Hg of 0.2 ng/L.

Major Elements, Specific Conductance and pH

Accumulation mode aerosols, characterized by a high light scattering efficiency and a long residence time in the atmosphere, have dry diameters ranging from 0.1 and 2.5 μm . Our samples were thawed and filtered to less than 0.45 μm at our laboratory in Fairbanks, Alaska, thereby eliminating the coarser aerosols but retaining a significant fraction of the smaller aerosol particles. Samples were allowed to thaw to 25°C inside polypropylene sample bags. The resulting water was split into three 60 mL aliquots for the measurement of: 1) major cation and anion concentrations, 2) specific conductance, and 3) pH.

Waters for major ions were filtered through precleaned 0.45 μm polypropylene filters and were split into two equal aliquots of 30 mL, one each for anions and cations. The waters for cation concentration measurements were acidified to pH~1 with the addition of trace element grade HNO_3 . Major ion concentrations were measured in the Department of Environmental Studies at Dartmouth College in Hanover, New Hampshire. Cations were measured using a Spectro Analytical Instruments SpectroFlame Inductively Coupled Plasma Optical Emission Spectrometer. Anions were measured using a Dionex DX

120 Ion Chromatograph. Multiple analyses of laboratory precipitation standards SLRS-4 (National Research Council of Canada) and P-31 (United States Geological Survey) indicate an analytical uncertainty of $\pm 2\%$ for ICP-OES analyses and $\pm 5\%$ for IC analyses (Table A1).

Non-sea salt SO_4^{2-} concentration, a proxy of arctic haze aerosols, was calculated by multiplying the measured sodium concentration in a sample by 0.2517 (the Na to SO_4^{2-} ratio in bulk seawater) and then subtracting the resulting value from the SO_4^{2-} concentration measured in the same sample.

Specific conductance was measured using a meter calibrated with 0, 10.76 and 100.1 $\mu\text{S}/\text{cm}$ standards. Multiple analyses of two low ionic strength standard reference samples yielded average specific conductances of 59.6 ± 0.9 and 10.7 ± 0.4 , within the 95% confidence interval of the most probable values (59.9 and 10.8, respectively). The average difference in measured specific conductance between the twelve duplicate samples taken from three different sample locations was 0.4 $\mu\text{S}/\text{cm}$.

Snowmelt pH was measured using a pH meter with automatic temperature compensation. The ionic strength of the melted snow sample was buffered with the addition of low ionic strength adjustor solution. During pH measurement the melted snow sample was slowly stirred while held isothermal at 25°C in a precleaned covered polyethylene beaker. The USGS low ionic strength precipitation standard P-31 was used to monitor the precision and accuracy of the pH measurements. The average pH ($n=20$) measured from this reference standard using our experimental protocols was 7.48 ± 0.05 , within the 95% confidence interval of the most probable value (7.44). The average difference in measured pH between the twelve duplicate samples taken from three different sample sites was 0.06.

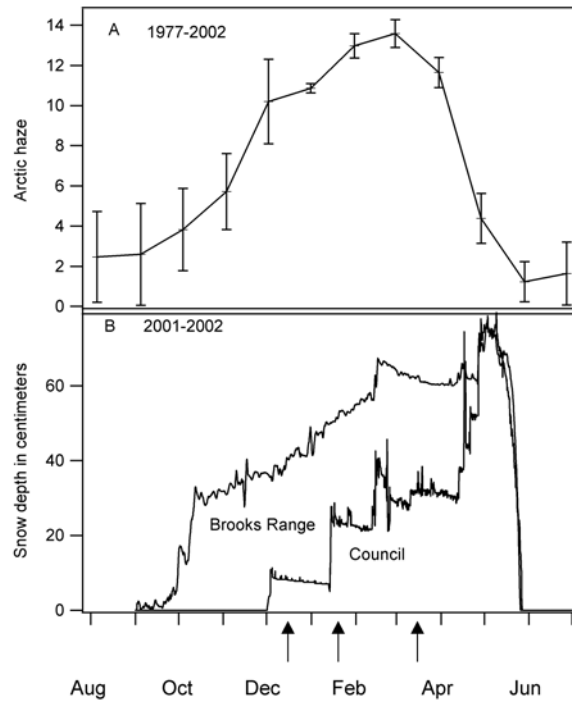


Figure 1. 8.5 cm X 10.5 cm; one column.

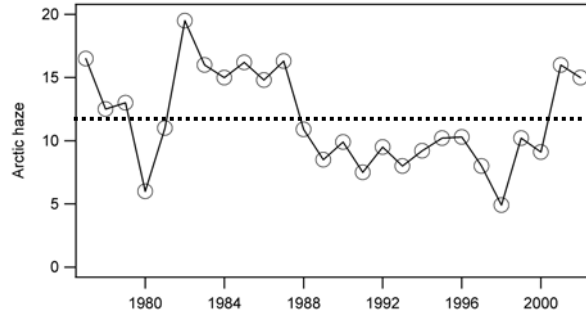


Figure 2. 8.5 cm X 4.5 cm; one column.

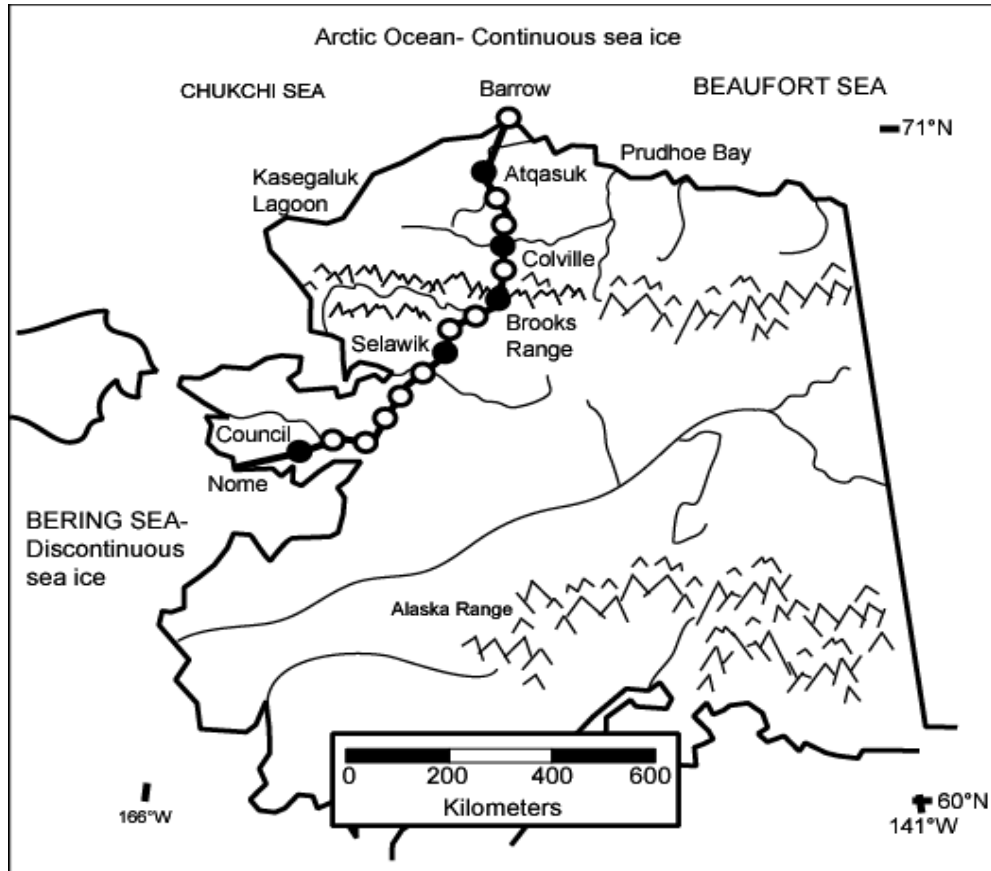


Figure 3. 14.5 cm X 13 cm; two columns

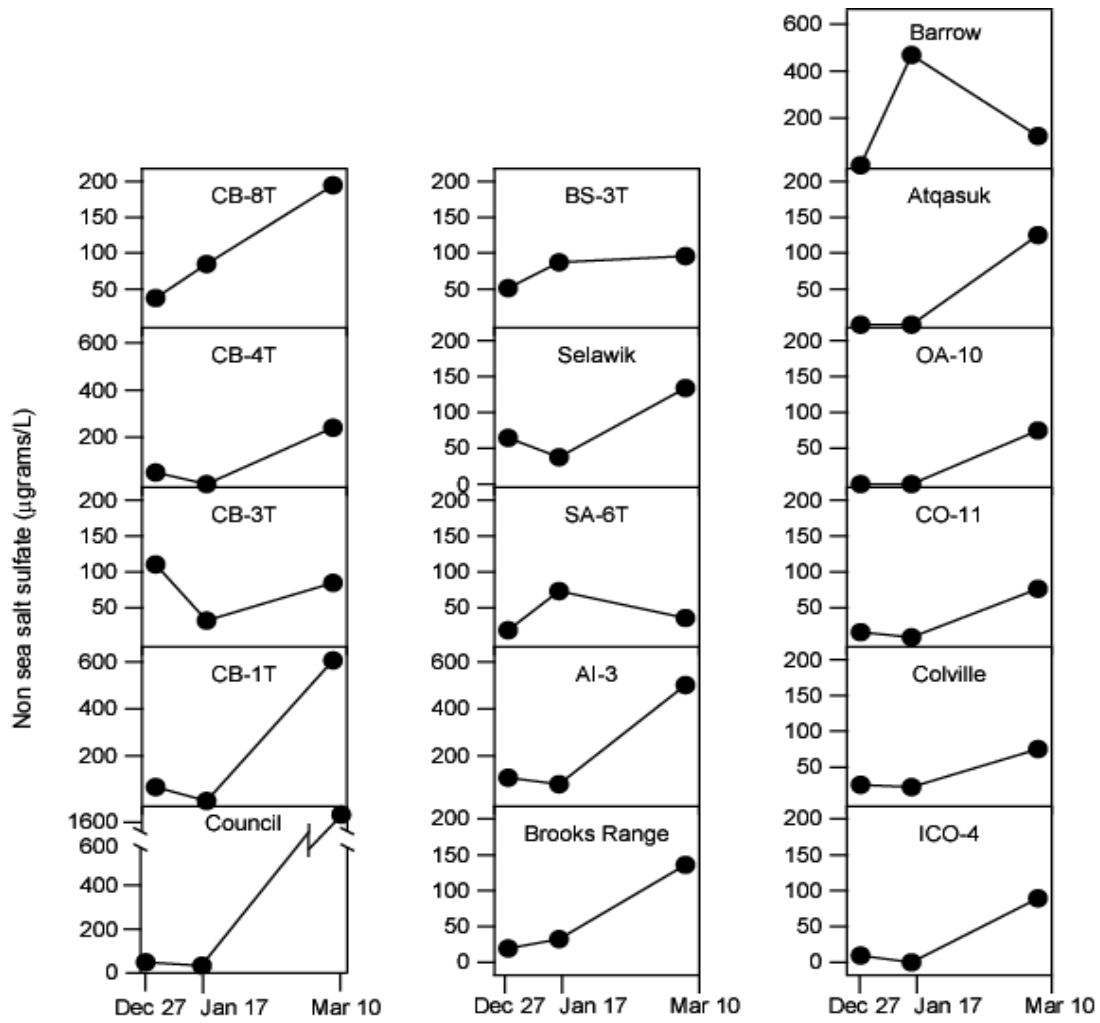


Figure 5. 15.5 cm X 15 cm; two columns

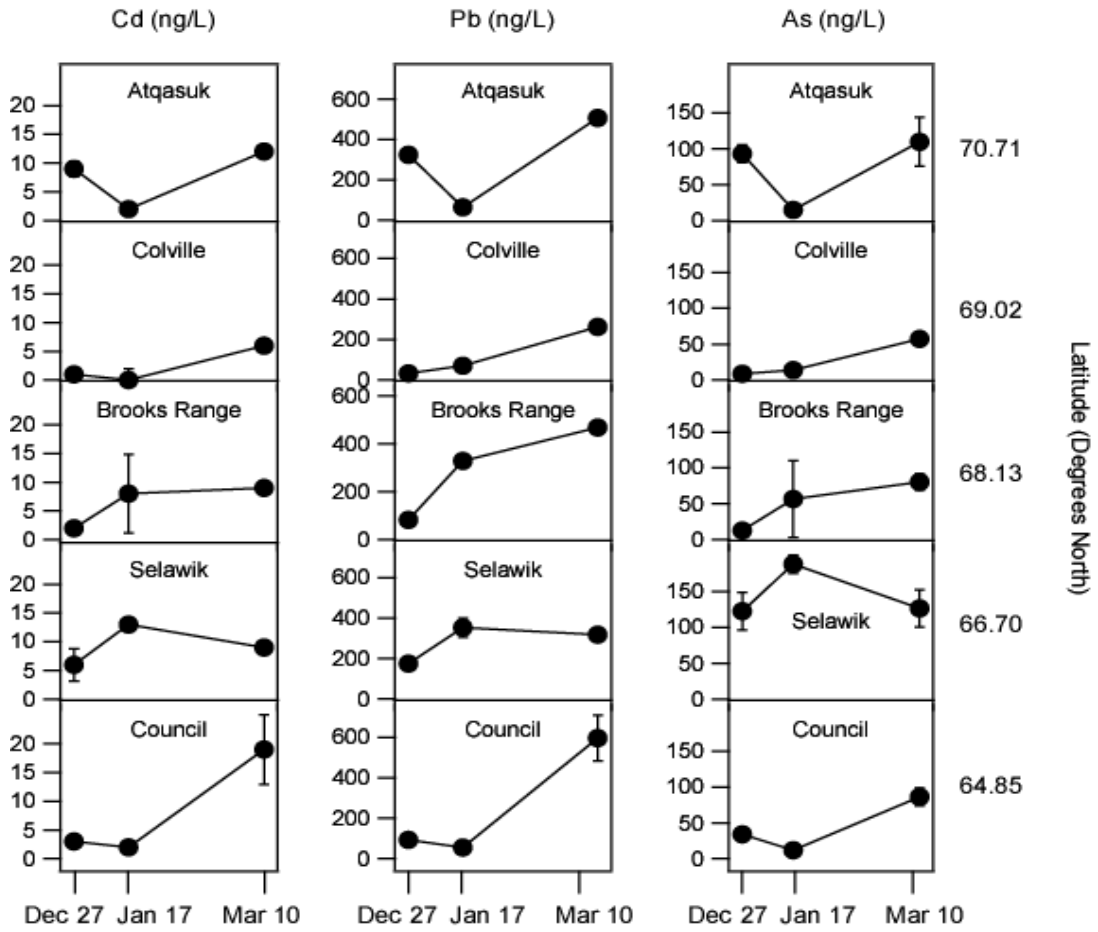


Figure 6. 16 cm X 14.5 cm; two columns

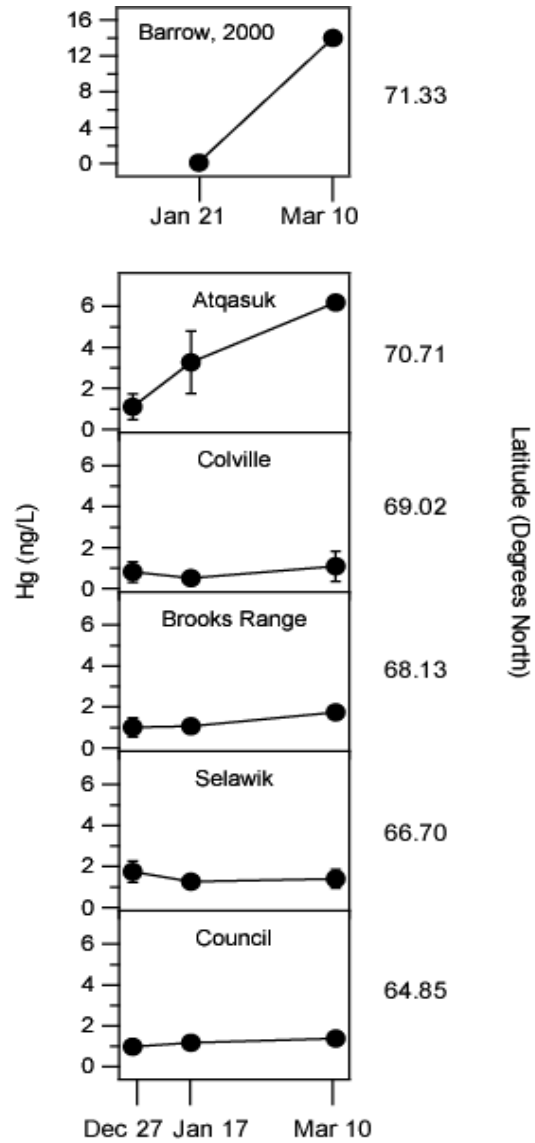


Figure 7. 8 cm X 15 cm; one column

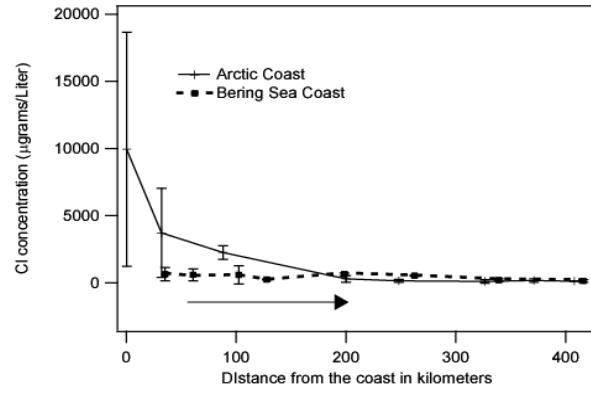


Figure 8. 8.5 cm X 7 cm; one column

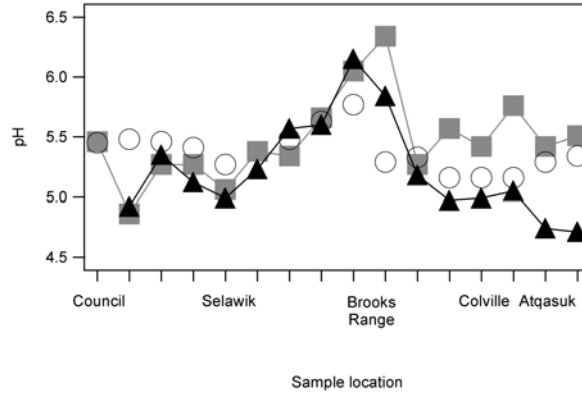


Figure 9. 8.5 cm X 5.5 cm; one column

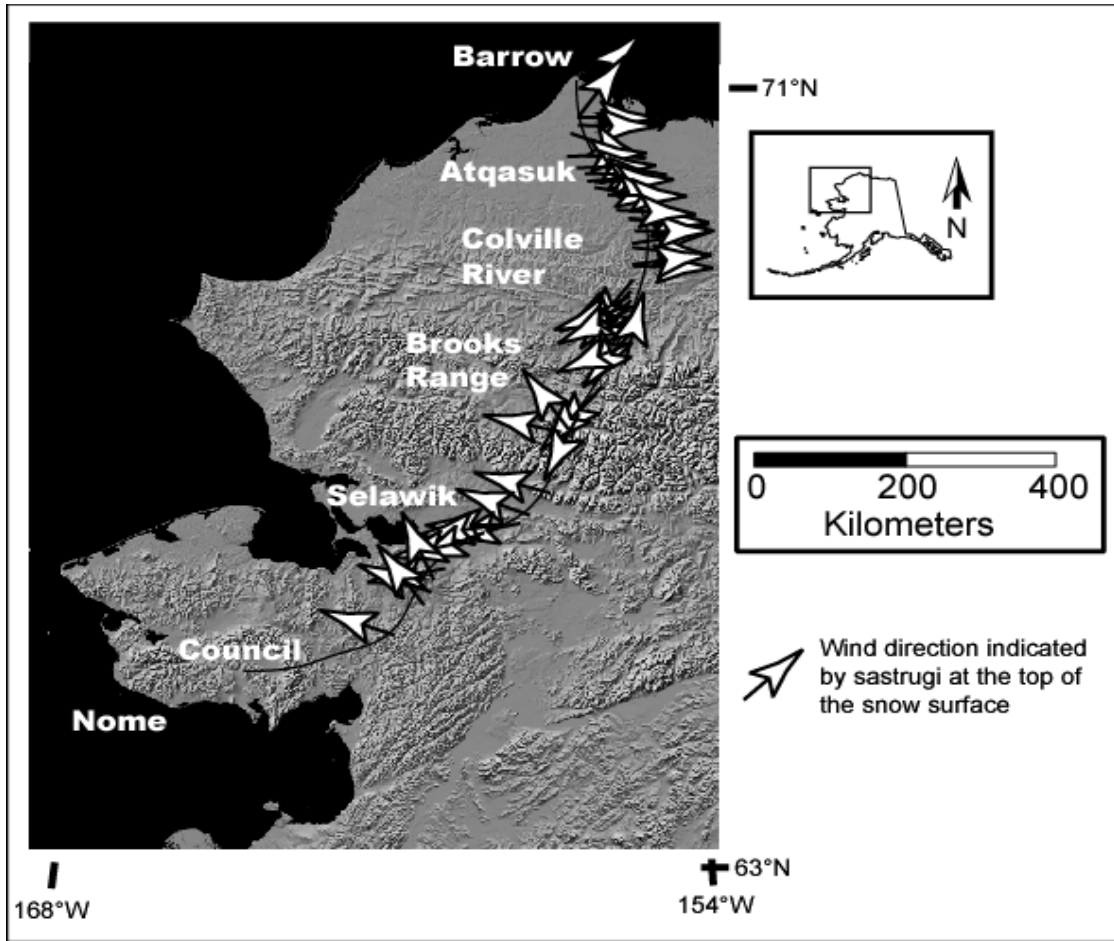


Figure 10. 16.5 cm X 14 cm; two columns